

TBF effect on off-shell mass operator and spectral functions in nuclear matter

Pei Wang,^{1,2} Sheng-Xin Gan,^{1,2} Peng Yin,^{1,2} and Wei Zuo^{1,*}

¹*Institute of Modern Physics, Chinese Academy of Sciences, Lanzhou 730000, China*

²*University of Chinese Academy of Sciences, Beijing 100049, China*

Abstract

Within the framework of the Brueckner theory, the off-shell behaviors of the mass operator $M(k, \omega) = V(k, \omega) + iW(k, \omega)$, i.e., its dependence upon the momentum k and upon the nucleon frequency ω , are investigated by including nuclear three-body force (TBF). The first two terms of the hole-line expansion of the mass operator are taken into account. The TBF effects on their off-shell properties are discussed. A comparison is made between the on-shell and off-shell values of M_1 . The nucleon spectral function and nucleon momentum distribution are also calculated, and the calculation shows that they are hardly affected by the TBF effect at the saturation density. At a high density two times greater than the saturation density, inclusion of the TBF may lead to a visible effect on the spectral function and may enhance the depletion of the hole states.

PACS numbers: 21.65.-f, 21.30.Fe, 24.10.Cn, 21.10.Pc

*zuowei@impcas.ac.cn

I. INTRODUCTION

The probability of removing a particle with momentum k from a target nuclear system, leaving the final system with excitation energy ω , is reflected by the nucleon spectral function $S(k, \omega)$. In the free Fermi gas model, the spectral function can be written as $S(k, \omega) = \delta(\omega - \hbar^2 k^2 / 2m)$. However, many-body correlations among the nucleons, induced by the nucleon-nucleon (NN) interactions, broaden the peaks of the Fermi-gas spectral function and decrease their strengths. It has been shown that, most of this decrease of the strength of the single-particle (s.p.) states with respect to the standard mean field estimates [1] is due to the NN correlations [2, 3], whose effects can be most accurately studied in infinite nuclear matter. Therefore, a microscopic calculation of the nucleon spectral function in nuclear matter is of special interest since it may play an important role in understanding the nature of the NN correlations, especially the short-range and tensor correlations [4, 5].

The interest in the spectral function has also been raised by the treatment of the off-shell effect in transport theory, which provides a generalized theoretical framework to describe the time evolution of heavy ion reactions. The use of the quasiparticle approximation (QPA) in transport theory puts the nucleon on the mass shell, neglecting not only the finite decay width of the particles, but also the width of the nucleon spectral function. However, the on-shell quasiparticle limit should not be adequate for particles with short lifetimes and/or high collision rates as recognized previously [6, 7]. Therefore, there have been attempts to go beyond the QPA, such as transport formulations for quasiparticles with dynamical spectral functions [8–10], and extend the extensively applied models [11–21]. The nucleon spectral function plays an important role in the implementation of the off-shell effects in a transport theoretical treatment of heavy-ion and other nuclear collisions.

Experimentally, the information about the nuclear spectral function and the effect of NN correlations in nuclear systems can be extracted from the $(e, e'p)$ and proton-induced knockout reactions [4, 5, 22–26]. Theoretically, the nuclear short-range correlations and the spectral function in nuclear matter have been investigated extensively by using various microscopic nuclear many-body approaches, such as the Green function theory [27–34], the correlated basis function method [35–38], the extended Brueckner-Hartree-Fock (EBHF) framework [39–43], and the in-medium T -matrix approach [44–46]. For a review, we refer readers to Refs. [4, 5]. Within the framework of the Brueckner theory, the nucleon spectral

function in symmetric nuclear matter has been studied in Ref. [41] by adopting a finite-rank representation of the realistic Argonne *V14* *NN* interaction, without taking into account any three-body force (TBF) effect. In Refs. [34, 43], the neutron and proton spectral functions in isospin-asymmetric nuclear matter have been explored using the BHF approach and the Green function theory, respectively. It is well known that inclusion of TBF in the nonrelativistic Brueckner theory is crucial for reproducing the nuclear saturation properties and for better describing the s.p. properties, such as the momentum dependence of the nucleon s.p. potential [47–50]. Recently, the TBF effect on the spectral function in nuclear matter has been investigated within the framework of the in-medium *T*-matrix method in Ref. [46], where the TBF adopted is the Urbana TBF [51]. In that paper, the authors have shown that the TBF effect on the spectral functions is quite small at low densities around and below the saturation density and that noticeable modification of the spectral functions is realized only for high densities well above the saturation density. One of our purposes in the present paper is to investigate the possible impact of a microscopic TBF on the nucleon spectral function within the framework of the extended BHF approach.

The spectral function is closely related to the mass operator $M(k, \omega)$, whose off-shell behavior is also our concern in the present paper. The off-shell mass operator plays an important role in the dispersion relation to the nuclear mean field [52] and in the discussion of *y*-scaling in inclusive electron scattering [53–55]. In Ref. [41], the properties of the off-shell mass operator have been obtained within the Brueckner theory in the absence of any TBF. Therefore, the other purpose of the present paper is to reveal the TBF effect on the off-shell mass operator discussed in Ref. [41].

The paper is organized as follows. In Sec. II, we give a brief review of the mass operator and spectral function, i.e., their definitions and physical interpretations, as presented in Ref. [41]. We also provide a simple introduction to the Brueckner theory and the microscopic TBF adopted in our calculation. In Secs. III and IV, we focus on the real and imaginary parts of the off-shell mass operator. We study the *k*-dependence of $M(k, \omega)$ for the two typical energies, $\omega = 20$ MeV and $\omega = 160$ MeV, at 0.34 fm^{-3} . We also calculate the ω -dependence of $M(k, \omega)$ for $k = \frac{3}{4}k_F$ and $k = \frac{5}{4}k_F$. The off-shell results of $M_1(k, \omega)$ are compared with the on-shell ones. The TBF effect on the *k* and ω -dependence of $M(k, \omega)$ is discussed. In Sec. V, we calculate the spectral function and investigate the TBF effect on its ω -dependence. In Sec. VI, a summary is given.

II. FORMALISM

A. The mass operator and the spectral function

The Green function in the energy-momentum representation is given by $G(k, \omega) = [\omega - k^2/2m - M(k, \omega)]^{-1}$, where $M(k, \omega) = V(k, \omega) + iW(k, \omega)$ is the mass operator that can be identified with the mean field felt by a nucleon in a nuclear system. The real and imaginary parts of the mass operator are connected by the dispersion relation [41]:

$$V(k, \omega) = \lim_{\omega \rightarrow \infty} V(k, \omega) + \frac{1}{\pi} \int_{-\infty}^{\infty} \frac{W(k, \omega')}{\omega' - \omega} d\omega' . \quad (1)$$

The spectral function is given by

$$S(k, \omega) = -\frac{1}{\pi} \left(\frac{W(k, \omega)}{[\omega - k^2/2m - V(k, \omega)]^2 + [W(k, \omega)]^2} \right) , \quad (2)$$

and it fulfills the sum rule

$$\int_{-\infty}^{\infty} S(k, \omega) d\omega = 1. \quad (3)$$

The occupation probability $n(k)$ is related to the spectral function by

$$n(k) = \int_{-\infty}^{\omega_F} S(k, \omega) d\omega \quad (4)$$

and

$$n(k) = 1 - \int_{\omega_F}^{\infty} S(k, \omega) d\omega . \quad (5)$$

The Fermi energy ω_F fulfills $\omega_F = k_F^2/2m + V(k_F, \omega_F)$. For a system of A nucleons, $S(k, E^*)$ measures the probability density of finding the residual $(A - 1)$ -nucleon system with excitation energy $E^* = \omega_F - \omega$ ($\omega < \omega_F$) after removing a nucleon with momentum k from the ground state, or the probability density of finding the residual $(A + 1)$ -nucleon system with the excitation energy $E^* = \omega - \omega_F$ ($\omega > \omega_F$) after one has added a nucleon with momentum k to the ground state.

B. Brueckner theory with a microscopic TBF

The starting point of Brueckner calculation of nuclear matter properties is to obtain the Brueckner reaction matrix $G(\omega)$ by solving the Bethe-Goldstone (BG) equation

$$G(\omega) = V_{\text{NN}} + V_{\text{NN}} \sum_{k_1 k_2} \frac{|k_1 k_2\rangle Q(k_1 k_2) \langle k_1 k_2|}{\omega - \epsilon(k_1) - \epsilon(k_2) + i\eta} G(\omega) , \quad (6)$$

where k_1 and k_2 are momenta of the two involved nucleons. $Q(k_1, k_2) = [1 - n(k_1)][1 - n(k_2)]$ is the Pauli operator which prevents two intermediate nucleons from being scattered into occupied states. ω is the starting energy. The single-particle energy $\epsilon(k)$ satisfies the on-shell relation $\epsilon(k) = k^2/2m + U_{\text{BHF}}(k)$, where the auxiliary potential $U_{\text{BHF}}(k)$ is the single-particle potential at the BHF level and it is defined as $U_{\text{BHF}}(k) = \sum_{k'} \text{Re} \langle kk' | G(\epsilon(k) + \epsilon(k')) | kk' \rangle_A$. The subscript A denotes antisymmetrization of the matrix element. The continuous choice other than gap choice is adopted when solving the BG equation to obtain the G -matrix [56].

Extension of the Brueckner-Bethe-Goldstone (BBG) theory to include TBFs can be found in Refs. [47, 48]. In this paper, we choose the microscopic TBF which is based on the meson-exchange current model proposed by P. Grangé *et al.* [57] and reduced to an equivalent effective two-body force V_3^{eff} via an average with respect to the third-nucleon degree of freedom. The effective force V_3^{eff} in r space reads

$$\begin{aligned} V_3^{\text{eff}}(\vec{r}'_1, \vec{r}'_2 | \vec{r}_1, \vec{r}_2) &= \frac{1}{4} \text{Tr} \sum_n \int d\vec{r}_3 d\vec{r}'_3 \phi_n^*(\vec{r}'_3) [1 - \eta(r'_{13})] \\ &\times [1 - \eta(r'_{23})] W_3(\vec{r}'_1, \vec{r}'_2, \vec{r}'_3 | \vec{r}_1, \vec{r}_2, \vec{r}_3) \\ &\times \phi_n(\vec{r}_3) [1 - \eta(r_{13})] [1 - \eta(r_{23})] , \end{aligned} \quad (7)$$

where the wave function ϕ_n denotes the single nucleon wave function in free space. The realistic NN interaction V_{NN} in the BG equation is the sum of the Argonne V_{18} (AV18) two-body interaction and the effective two-body force V_3^{eff} , as described in Refs. [47, 48]. Since $\eta(r)$ in expression (7) is the so-called defect function [57, 58] corresponding to the G -matrix, V_3^{eff} should be recalculated along with the G -matrix in each iteration of our BHF procedure to ensure self-consistency of the BG equation.

In the spirit of Brueckner theory, the first two terms of the hole-line expansion of the mass operator are the BHF approximation $M_1(k, \omega)$ and the Pauli rearrangement correction $M_2(k, \omega)$. They are represented by the diagrams of Fig.1, and their expressions read :

$$M_1(k, \omega) = \sum_{h < k_F} \langle kh | G[\omega + \epsilon(h)] | kh \rangle_A, \quad (8)$$

$$M_2(k, \omega) = \frac{1}{2} \sum_{l, m < k_F, n > k_F} \frac{|\langle lm | G[\epsilon(l) + \epsilon(m)] | kn \rangle_A|^2}{\omega + \epsilon(n) - \epsilon(l) - \epsilon(m) - i\delta}. \quad (9)$$

Their off-shell values can be calculated as long as the G -matrix is obtained.

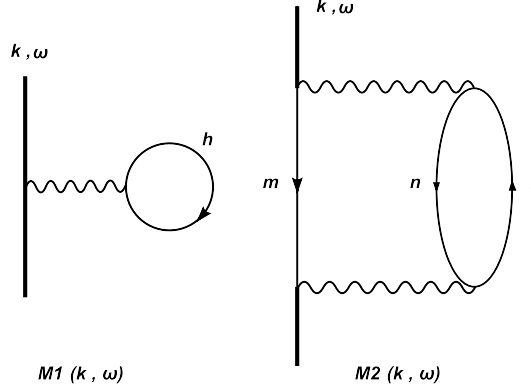


FIG. 1: Representation of the first two terms of the hole-line expansion of the mass operator. The thin lines represent either particle (upward-pointing arrows) or hole (downward-pointing arrows) momentum states. The thick lines show the values of the nucleon momentum k and frequency ω .

III. FREQUENCY DEPENDENCE OF THE MASS OPERATOR AT FIXED MOMENTUM

A. Real part of the off-shell mass operator

The calculated ω -dependence of $V_1(k, \omega) = \text{Re}M_1(k, \omega)$ and $V_2(k, \omega) = \text{Re}M_2(k, \omega)$ is shown in Fig. 2 for the two densities of $\rho = 0.17 \text{ fm}^{-3}$ and $\rho = 0.34 \text{ fm}^{-3}$, respectively. Two fixed momenta ($k = \frac{3}{4}k_F$ and $k = \frac{5}{4}k_F$) are selected. The quantity e_F is the calculated value of the single-particle energy $\epsilon(k)$ at the Fermi momentum: $e_F = \epsilon(k_F) = k_F^2/2m + U_{\text{BHF}}(k_F)$. As one can see in Fig. 2, the quantity $V_1(k, \omega)$ is attractive for $\omega < e_F$ and its attraction increases as a function of frequency ω in the region of $\omega < e_F$, while $V_2(k, \omega)$ is repulsive for $\omega > e_F$ and its repulsion decreases with increasing ω in the region of $\omega > e_F$. The TBF effect on their ω -dependence is also reported in this figure. Inclusion of the TBF in our calculations hardly affects the ω -dependence of $V_2(k, \omega)$, but tends to reduce the attraction of $V_1(k, \omega)$ well below e_F and enhance its attraction as ω is much larger than e_F . At the saturation density of 0.17 fm^{-3} , the TBF effect on $V_1(k, \omega)$ is weak enough to be neglected in the vicinity of e_F . However, the TBF effect gets much stronger at high densities. As a result, the TBF-induced reduction of the attraction of $V_1(k, \omega)$ well below e_F is obviously seen at two times the saturation density 0.34 fm^{-3} , as revealed in the right panel of Fig. 2. At high densities, the TBF effect on V_2 turns out to be rather small. At $\rho = 0.34 \text{ fm}^{-3}$ and

$k = 2.1\text{fm}^{-1}$, inclusion of the TBF may enhance slightly the repulsion of V_2 .

Besides, it is worth noticing that the distinct deviation of the curve with open squares from that with filled squares when $\omega - e_F$ is above 150 MeV. The deviation appears regardless of the density value, which indicates that one should account for the TBF effect carefully in the high-energy domain.

B. Imaginary part of the off-shell mass operator

Figure 3 shows the dependence of $W_1(k, \omega)$ and $W_2(k, \omega)$ upon the difference $\omega - e_F$. One important feature of the two components is that $W_1(k, \omega)$ vanishes for $\omega < e_F$ and $W_2(k, \omega)$ vanishes for $\omega > e_F$. Moreover, $W_2(k, \omega)$ also vanishes for large negative ω . At the saturation density of 0.17 fm^{-3} , the calculated $W_1(k, \omega)$ including the TBF contribution is very close to its values without including the TBF contribution in the energy domain ranging from e_F to approximately 300 MeV. However, as density increases to 0.34 fm^{-3} where the TBF effect becomes strong, inclusion of the TBF leads to a faster increase of the attraction of $W_1(k, \omega)$ with increasing frequency ω as compared to the result without the TBF effect. At $\rho = 0.34\text{fm}^{-3}$ and $k = 2.1\text{fm}^{-1}$, inclusion of the TBF may lead to a sizable enhancement of the attraction of W_2 .

C. Comparison with on-shell values

In Fig. 4, we compare the off-shell values of $W_1(k, \omega)$ and $W_2(k, \omega)$ with their on-shell values. Although our calculations are done at a higher density of 0.34 fm^{-3} and in the presence of the TBF, the results plotted in Fig. 4 are similar qualitatively to those in Fig. 12 of Ref. [41], regardless of the magnitude. Therefore, the analysis and conclusion in Ref. [41] remain valid. That is to say, on the one hand, $W_1(k, \omega)$ and $W_2(k, \omega)$ are symmetric with each other only in the vicinity of the Fermi energy; on the other hand, the assumption in the simplest version of the dispersion relation approach for the nuclear mean field [i.e., the ω -dependence of $W_1(k, \omega)$ is approximated by the e -dependence of the on-shell $W_1(e)$] is only justified qualitatively.

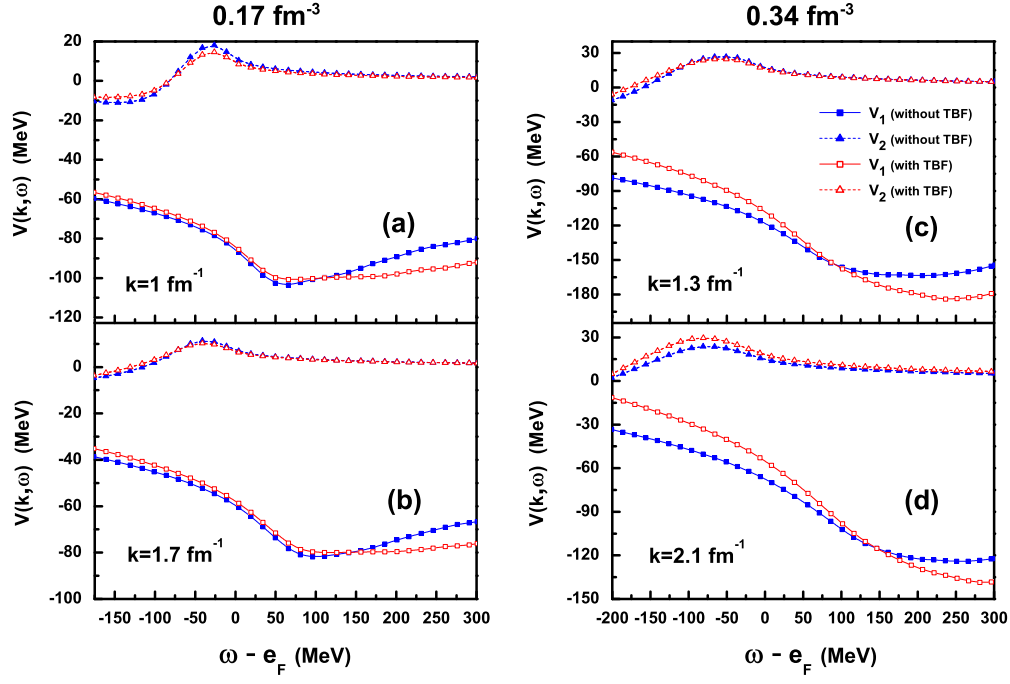


FIG. 2: (Color online) Dependence of $V_1(k, \omega)$ and $V_2(k, \omega)$ upon $\omega - e_F$ for the two densities of $\rho = 0.17 \text{ fm}^{-3}$ and $\rho = 0.34 \text{ fm}^{-3}$, and for the two fixed momenta of $k = \frac{3}{4}k_F$ and $k = \frac{5}{4}k_F$. The curves with open squares and open triangles have taken into account the TBF contribution.

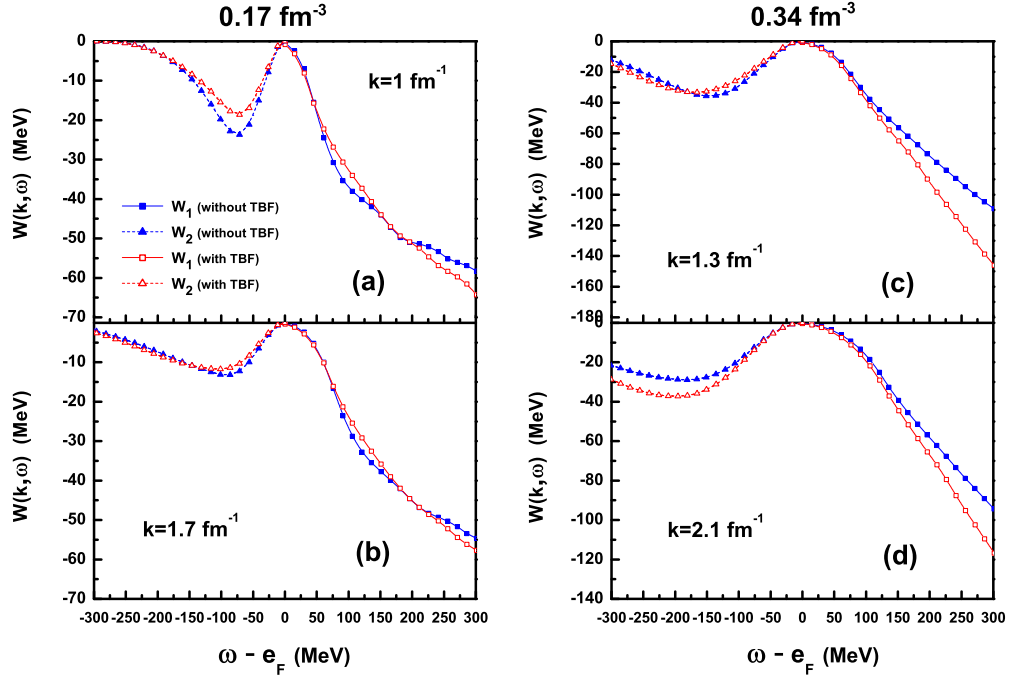


FIG. 3: (Color online) Dependence of $W_1(k, \omega)$ and $W_2(k, \omega)$ upon $\omega - e_F$ for the two densities of $\rho = 0.17 \text{ fm}^{-3}$ and $\rho = 0.34 \text{ fm}^{-3}$, and for the two fixed momenta of $k = \frac{3}{4}k_F$ and $k = \frac{5}{4}k_F$. The

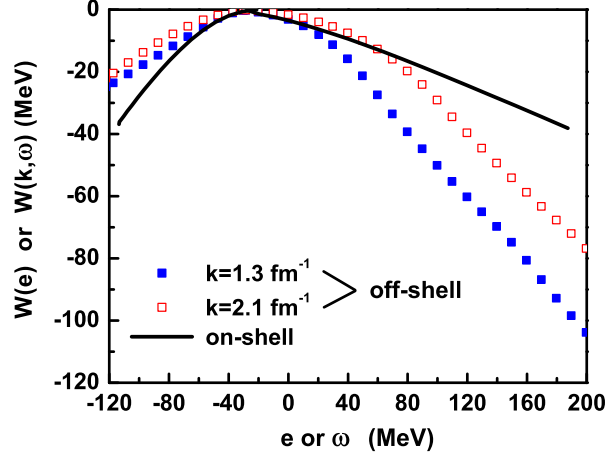


FIG. 4: (Color online) Comparison between the e -dependence of the on-shell $W_1(e)$ and $W_2(e)$ (solid curve) with the ω -dependence of $W_1(k, \omega)$ and of $W_2(k, \omega)$, for $k = 1.3 \text{ fm}^{-1}$ (filled squares) and $k = 2.1 \text{ fm}^{-1}$ (open squares), at the density of 0.34 fm^{-3} .

IV. MOMENTUM DEPENDENCE OF THE BHF FIELD $M_1(k, \omega)$ AT FIXED FREQUENCY

At the density of 0.34 fm^{-3} , we calculate the dependence of $V_1(k, \omega)$ and $W_1(k, \omega)$ upon momentum k for two fixed frequencies, namely $\omega_1 = 20 \text{ MeV}$ and $\omega_2 = 160 \text{ MeV}$. The corresponding on-shell values of the momentum, which can be obtained from the energy-momentum relation $\omega(k) = k^2/2m + V[k, \omega(k)]$, are approximately $k(\omega_1) = 2.15 \text{ fm}^{-1}$ and $k(\omega_2) = 3.15 \text{ fm}^{-1}$. Results for the saturation density 0.17 fm^{-3} are not provided, because the TBF effect is not expected to play an important role at such a relatively low density.

In Fig. 5, the upper part displays the calculated values of $V_1(k, \omega = 20 \text{ MeV})$ and $V_1(k, \omega = 160 \text{ MeV})$; the lower part presents the calculated values of $W_1(k, \omega = 20 \text{ MeV})$ and $W_1(k, \omega = 160 \text{ MeV})$.

As we can see from the figure, for both the real and the imaginary parts of $M_1(k, \omega)$, the open squares are very close to the corresponding filled squares in the high momentum region, indicating that the TBF correction is small at high momenta. However, in the low momentum region, the TBF has a strong effect on the shape of the k -dependence of $V_1(k, \omega)$ and $W_1(k, \omega)$ only at the larger frequency $\omega = 160 \text{ MeV}$, and it may separate the open

squares and the corresponding filled ones considerably. As a result, it is necessary to take into account the TBF effect if one wants to get more exact and reliable k -dependence of the off-shell mean field $M_1(k, \omega)$ felt by a nucleon with both low momentum and large frequency.

V. SPECTRAL FUNCTION

The spectral function $S(k, \omega)$ can be calculated from Eq.(2), using the real and imaginary parts of the mass operator. Notice that in the present approximation scheme, $W(k, \omega) = W_2(k, \omega)$ for $\omega < e_F$ and $W(k, \omega) = W_1(k, \omega)$ for $\omega > e_F$. For energies $\omega < e_F$, the spectral function $S(k, \omega)$ is referred to as the “hole spectral function” $S_h(k, \omega)$, and for energies $\omega > e_F$, the $S(k, \omega)$ becomes the “particle spectral function” $S_p(k, \omega)$. $S_{h(p)}(k, \omega)$ measures the probability that a nucleon with momentum k and energy ω can be removed from (added to) the ground state.

In Fig. 6, the spectral function is plotted versus ω at the density of 0.34 fm^{-3} . The upper part of the figure displays the spectral distribution for momentum below the Fermi momentum. In the independent-particle model, states with momenta below the Fermi surface would be completely occupied so that the spectral function is identical to a δ function located at the on-shell value of ω . However, the two-hole configuration leads to a non vanishing imaginary part of the mass operator and consequently a finite spectral function peaked at the on-shell energy for momenta below k_F [4, 5]. The quasiparticle peak in the spectral function can be related to the shell model by the fact that when a nucleon with momentum k is removed from the ground state, the residual system has a large probability of having a well-defined excitation energy E_{A-1}^* [41]. The lower part of the figure shows the spectral distribution for momentum above k_F .

Recently, the TBF effect on the spectral function in nuclear matter has been investigated explicitly within the in-medium T -matrix method in Ref. [46] where the Urbana TBF [51] has been adopted. One may notice from the upper panel of Fig. 6 that, at momentum below the Fermi momentum k_F , the TBF effect on the spectral distribution leads to a shift of the peak location to slightly higher energy and a decrease in the peak value, in agreement with the results of Ref. [46] within the in-medium T -matrix method using the Urbana TBF. It is also seen that the TBF reduces the strength of the spectral distribution at large negative energies. At momentum above k_F , the TBF effect is mainly to shift the

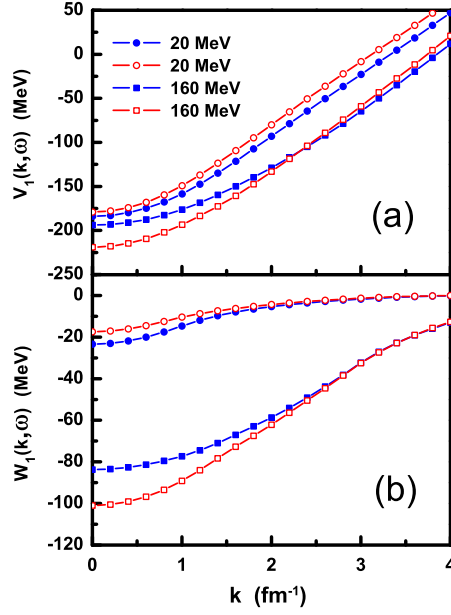


FIG. 5: (Color online) Dependence upon k of the calculated values of $V_1(k, \omega)$ and of $W_1(k, \omega)$ for the two selected frequencies: $\omega = 20$ MeV and $\omega = 160$ MeV. Open symbols correspond to the case with TBF contribution, while filled symbols do not. The density is fixed at 0.34 fm^{-3} .

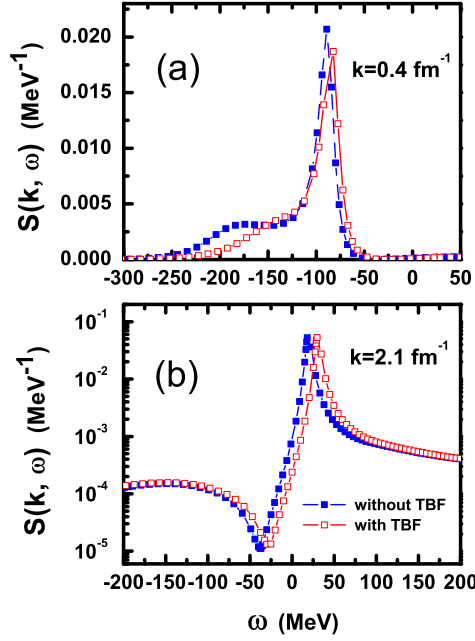


FIG. 6: (Color online) Spectral function $S(k, \omega)$ calculated from Eq.(2) at the density of 0.34 fm^{-3} .

peak value to a higher energy. The TBF-induced shift of the peak location of the spectral distribution can be understood readily since the TBF gives an extra repulsive contribution to the on-shell single-particle potential and consequently increases the on-shell energy for a given momentum k .

In order to test the numerical accuracy of the present work, in Fig. 7 we display the nucleon momentum distribution defined in Eq. (4) for two densities $\rho = 0.17$ and 0.34fm^{-3} . By using Eq. (5) we get almost the same results. Due to the nucleon-nucleon correlations, the s.p. hole states below k_F are partly empty and the particle states above k_F are partly occupied in the correlated ground state of nuclear matter. The depletion of the lowest hole state at $k = 0$ at $\rho = 0.17\text{fm}^{-3}$ is about 16.4%, which is compatible with the previous predictions in Refs. [5, 34, 35, 37, 40, 42]. This value is also consistent with the experimental

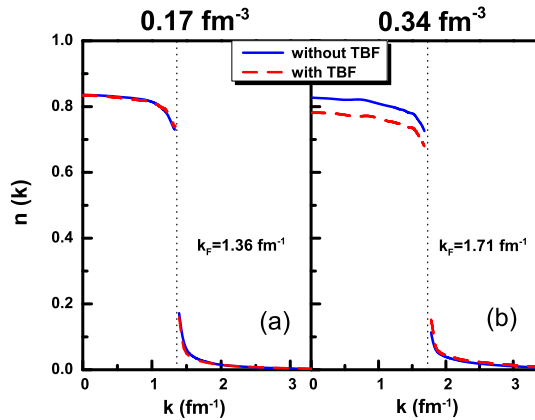


FIG. 7: (Color online) Nucleon momentum distribution in symmetric nuclear matter at two densities $\rho = 0.17 \text{ fm}^{-3}$ (left panel) and $\rho = 0.34 \text{ fm}^{-3}$ (right panel)

result in Ref. [26]. As discussed in Ref. [40], inclusion of the (higher order) renormalization contribution M_3 in the mass operator may reduce the calculated depletion from $\sim 17\%$ to $\sim 14\%$ by using a separable $AV14$ interaction. It is noticed that the TBF effect is negligibly small at the saturation density $\rho = 0.17\text{fm}^{-3}$, in agreement with the conclusion of Ref. [35] within the correlated basis function approach by adopting the Urbana $v14$ interaction plus an effective TBF. The TBF effect only becomes sizable at high densities well above the saturation density as shown in the right panel of Fig. 7 where the momentum distribution for $\rho = 0.34 \text{ fm}^{-3}$ is plotted. The TBF effect is shown to enhance the depletion of the

hole states since the TBF may induce sufficiently strong extra short-range correlations at sufficiently high densities. At $\rho = 0.34 \text{ fm}^{-3}$, inclusion of the TBF may enhance the depletion of the zero-momentum state from $\sim 17\%$ to $\sim 22\%$.

VI. SUMMARY

Within the framework of Brueckner theory extended to include a microscopic TBF, we have calculated the dependence of the off-shell mass operator upon the momentum k and upon the nucleon frequency ω . The first two terms in the hole-line expansion of the mass operator are taken into account. Our calculations show that the TBF effect on the values of $M_1(k, \omega)$ for fixed momentum is only important at high densities or at frequencies far away from its on-shell energy at k_F . However, the ω -dependence of the Pauli rearrangement term $M_2(k, \omega)$ at fixed momenta is even less affected by the TBF effect. At $\rho = 0.34 \text{ fm}^{-3}$ which is well above the saturation density, inclusion of the TBF may enhance the repulsion of V_2 at a large momentum $k = 2.1 \text{ fm}^{-1}$ above k_F . We also compare the off-shell values of M_1 at fixed momenta with its on-shell values. For fixed frequency, the k -dependence of the BHF field M_1 is investigated, and it is shown that it is necessary to take into account the TBF effect if one wants to get a more exact k -dependence of the mean field $M_1(k, \omega)$ felt by a nucleon with both low momentum and large frequency. The nucleon spectral function has been calculated. At density of $\rho = 0.34 \text{ fm}^{-3}$ well above the saturation density, the TBF effect shifts the peak location in the spectral function to slightly higher energy and reduces slightly the peak value at low momentum below the Fermi momentum k_F . The TBF effect on the nucleon spectral function and nucleon momentum distribution turns out to be neglected at the saturation density $\rho = 0.17 \text{ fm}^{-3}$. It becomes sizable only at high densities well above the saturation density, and inclusion of the TBF leads to an enhancement of the depletion of the zero-momentum hole state from $\sim 17\%$ to $\sim 22\%$ at $\rho = 0.34 \text{ fm}^{-3}$.

Acknowledgments

The work is supported by the National Natural Science Foundation of China (Grant No. 11175219), the Major State Basic Research Developing Program of China (Grant No. 2013CB834405), the Knowledge Innovation Project (Grant No. KJCX2-EW-N01) of Chi-

nese Academy of Sciences, the Chinese Academy of Sciences via a grant for visiting senior international scientists (Grant No. 2009J2-26), the Project of Knowledge Innovation Program (PKIP) of Chinese Academy of Sciences (Grant No. KJCX2.YW.W10), and the CAS/SAFEA International Partnership Program for Creative Research Teams (Grant No. CXTD-J2005-1).

- [1] B. Frois, and C. N. Papanicolas, *Ann. Rev. Nucl. Part. Sci.* **25**, 1 (1975).
- [2] S. Fantoni, and V. R. Pandharipande, *Nucl. Phys.* **A427**, 473 (1984).
- [3] V. R. Pandharipande, C. N. Papanicolas, and J. Wambach, *Phys. Rev. Lett.* **53**, 1133 (1984).
- [4] V. R. Pandharipande, I. Sick, and P. K. A. de Witt Huberts, *Rev. Mod. Phys.* **69**, 981 (1997).
- [5] W. Dickhoff, and C. Barbieri, *Prog. Part. Nucl. Phys.* **52**, 377 (2004).
- [6] W. Cassing, and S. J. Wang, *Z. Phys.* **A337**, 1 (1990).
- [7] R. Malfliet, *Prog. Part. Nucl. Phys.* **21**, 207 (1988).
- [8] P. A. Henning, *Nucl. Phys.* **A582**, 663 (1995).
- [9] P. A. Henning, *Phys. Rep.* **253**, 235 (1995).
- [10] R. Fauser, and H. Wolter, *Nucl. Phys.* **A584**, 604 (1995).
- [11] G. F. Bertsch, and S. Das Gupta, *Phys. Rep.* **160**, 189 (1988).
- [12] W. Cassing, V. Metag, U. Mosel, and K. Niita, *Phys. Rep.* **188**, 363 (1990).
- [13] C. M. Ko, and G. Q. Li, *J. Phys. G: Nucl. Part. Phys.* **22**, 1673 (1996).
- [14] J. Aichelin, *Phys. Rep.* **202**, 233 (1991).
- [15] G. Q. Li, A. Faessler, and S. W. Huang, *Prog. Part. Nucl. Phys.* **30**, 159 (1993).
- [16] B. A. Li, and C. M. Ko, *Phys. Rev. C* **52**, 2037 (1995).
- [17] S. H. Kahana, D. E. Kahana, Y. Pang, and T. J. Schlagel, *Ann. Rev. Nucl. Part. Sci.* **46**, 31 (1996).
- [18] W. Ehehalt, and W. Cassing, *Nucl. Phys.* **A602**, 449 (1996).
- [19] C. Grégoire, B. Remaud, and F. Sébille, L. Vinet, and Y. Raffray, *Nucl. Phys.* **A465**, 317 (1987).
- [20] H. Sorge, H. Stöcker, and W. Greiner, *Ann. Phys.* **192**, 266 (1989).
- [21] S. A. Bass, M. Belkacem, M. Bleicher, M. Brandstetter, L. Bravina, C. Ernst, L. Gerland,

- M. Hofmann, S. Hofmann, J. Konopka, G. Mao, L. Neise, S. Soff, C. Spieles, H. Weber, L. A. Winkelmann, H. Stocker, W. Greiner, Ch. Hartnack, J. Aichelin, and N. Amelin, Prog. Part. Nucl. Phys. **41**, 255 (1998).
- [22] W. H. Dickhoff, and M. M  ther, Rep. Prog. Phys. **55**, 1947 (1992).
- [23] P. K. A. de Witt Huberts, J. Phys. G **16**, 507 (1990).
- [24] L. Lapik  s, J. Wesseling, and R. B. Wiringa, Phys. Rev. Lett. **82**, 4404 (1999).
- [25] R. Starink, M. F. van Batenburg, E. Cisbani, W. H. Dickhoff, S. Frullani, F. Garibaldi, C. Giusti, D. L. Groep, P. Heimberg, W. H. A. Hesselink, M. Iodice, E. Jans, L. Lapikas, R. De Leo, C. J. G. Onderwater, F. D. Pacati, R. Perrino, J. Ryckebusch, M. F. M. Steenbakkens, J. A. Templon, G. M. Urciuoli, and L. B. Weinstein, Phys. Lett. **B474**, 33 (2000).
- [26] M. F. van Batenburg, Ph. D. thesis, University of Utrecht (2001).
- [27] A. Ramos, A. Polls, and W. H. Dickhoff, Nucl. Phys. **A503**, 1 (1989).
- [28] B. E. Vonderfecht, W. H. Dickhoff, A. Polls, and A. Ramos, Phys. Rev. C **44**, R1265 (1991).
- [29] B. E. Vonderfecht, W. H. Dickhoff, A. Polls, and A. Ramos, Nucl. Phys. **A555**, 1 (1993).
- [30] H. M  ther, G. Knehr, and A. Polls, Phys. Rev. C **52**, 2955 (1995).
- [31] Y. Dewulf, D. Van Neck, and M. Waroquier, Phys. Rev. C **65**, 054316 (2002); Y. Dewulf, W. H. Dickhoff, D. Van Neck, E. E. Stoddard, and M. Waroquier, Phys. Rev. Lett. **90**, 152501 (2003).
- [32] A. E. L. Dieperink, Y. Dewulf, D. Van Neck, M. Waroquier, and V. Rodin, Phys. Rev. C **68**, 064307 (2003).
- [33] T. Frick, H. M  ther, A. Rios, A. Polls, and A. Ramos, Phys. Rev. C **71**, 014313 (2005).
- [34] A. Rios, A. Polls, and I. Vidana, Phys. Rev. C **79**, 025802 (2009); A. Rios, A. Polls, and W. H. Dickhoff, Phys. Rev. C **79**, 064308 (2009).
- [35] S. Fantoni, and V. R. Pandharipande, Nucl. Phys. **A427**, 473 (1984).
- [36] O. Benhar, A. Fabrocini, and S. Fantoni, Nucl. Phys. **A505**, 267 (1989).
- [37] O. Benhar, A. Fabrocini, and S. Fantoni, Phys. Rev. C **41**, R24 (1990).
- [38] O. Benhar, A. Fabrocini, and S. Fantoni, Nucl. Phys. **A550**, 201 (1992).
- [39] M. Baldo, I. Bombaci, G. Giansiracusa, U. Lombardo, C. Mahaux, and R. Sartor, Phys. Rev. C **41**, 1748 (1990).
- [40] M. Baldo, I. Bombaci, G. Giansiracusa, and U. Lombardo, Nucl. Phys. **A530** 135 (1991).
- [41] M. Baldo, I. Bombaci, G. Giansiracusa, U. Lombardo, C. Mahaux, and R. Sartor, Nucl. Phys.

- A545**, 741 (1992).
- [42] T. Frick, Kh. Gad, H. Mütter, and P. Czerski, Phys. Rev. C **65**, 034321 (2002).
 - [43] Kh. S. A. Hassaneen, and H. Mütter, Phys. Rev. C **70**, 054308 (2004).
 - [44] P. Bozek, Phys. Rev. C **59**, 2619 (1999).
 - [45] P. Bozek, Phys. Rev. C **65**, 054306 (2002).
 - [46] V. Soma, and P. Bozek, Phys. Rev. C **78**, 054003 (2008).
 - [47] W. Zuo, A. Lejeune, U. Lombardo, and J.F. Mathiot, Nucl. Phys. **A706**, 418 (2002).
 - [48] W. Zuo, A. Lejeune, U. Lombardo, and J.F. Mathiot, Eur. Phys. J. **A14**, 469 (2002).
 - [49] W. Zuo, L. G. Cao, B. A. Li, U. Lombardo, and C. W. Shen, Phys. Rev. C **72**, 014005 (2005).
 - [50] M. Baldo, and C. Maieron, J. Phys. **G34**, R243 (2007).
 - [51] J. Carlson, V. Pandharipande, and R. Wiringa, Nucl. Phys. **A401**, 59 (1983).
 - [52] C. Mahaux, and R. Sartor, Nucl. Phys. **A528**, 253 (1991).
 - [53] X. D. Ji, and R. D. McKeown, Phys. Lett. **B236**, 130 (1990).
 - [54] C. Ciofi degli Atti, S. Liuti, and S. Simula, Phys. Rev. C **41**, R2474 (1990).
 - [55] T. Uchimaya, A. E. L. Dieperink, and O. Scholten, Phys. Lett. **B233**, 31 (1989).
 - [56] J. P. Jeukenne, A. Lejeune, and C. Mahaux, Phys. Rep. **25**, 83 (1976).
 - [57] P. Grangé, A. Lejeune, M. Martzolff, and J.F. Mathiot, Phys. Rev. C **40**, 1040 (1989).
 - [58] B. S. Pudliner, V. R. Pandharipande, J. Carlson, and R. B. Wiringa, Phys. Rev. Lett. **74**, 4396 (1995); B. S. Pudliner, V. R. Pandharipande, J. Carlson, S. C. Pieper, and R. B. Wiringa, Phys. Rev. C **56**, 1720 (1997).